
NANOCRYSTAL

Edited by **Yoshitake Masuda**

INTECHWEB.ORG

Nanocrystal

Edited by Yoshitake Masuda

Published by InTech

Janeza Trdine 9, 51000 Rijeka, Croatia

Copyright © 2011 InTech

All chapters are Open Access articles distributed under the Creative Commons Non Commercial Share Alike Attribution 3.0 license, which permits to copy, distribute, transmit, and adapt the work in any medium, so long as the original work is properly cited. After this work has been published by InTech, authors have the right to republish it, in whole or part, in any publication of which they are the author, and to make other personal use of the work. Any republication, referencing or personal use of the work must explicitly identify the original source.

Statements and opinions expressed in the chapters are these of the individual contributors and not necessarily those of the editors or publisher. No responsibility is accepted for the accuracy of information contained in the published articles. The publisher assumes no responsibility for any damage or injury to persons or property arising out of the use of any materials, instructions, methods or ideas contained in the book.

Publishing Process Manager Silvia Vlase

Technical Editor Teodora Smiljanic

Cover Designer Martina Sirotic

Image Copyright Leigh Prather, 2010. Used under license from Shutterstock.com

First published May, 2011

Printed in India

A free online edition of this book is available at www.intechopen.com
Additional hard copies can be obtained from orders@intechweb.org

Nanocrystal, Edited by Yoshitake Masuda

p. cm.

ISBN 978-953-307-199-2

INTECH OPEN ACCESS
PUBLISHER

INTECH open

free online editions of InTech
Books and Journals can be found at
www.intechopen.com

Contents

Preface IX

Part 1 Synthesis and Design of Nanocrystals 1

- Chapter 1 **Morphology Control of Metal Oxide Nanocrystals** 3
Yoshitake Masuda
- Chapter 2 **Size- and Shape-Controlled Synthesis of Monodisperse Metal Oxide and Mixed Oxide Nanocrystals** 55
Thanh-Dinh Nguyen and Trong-On Do
- Chapter 3 **Colloidal Hybrid Nanocrystals: Synthesis, Properties, and Perspectives** 85
Jie Zeng, Xiaoping Wang and J. G. Hou
- Chapter 4 **Nanocrystals in Metallic Glasses** 111
Rainer J. Hebert
- Chapter 5 **Preparation of Nano $\text{Al}_5\text{O}_6\text{N}$ via Shock Wave Plasmas Technique** 137
Zuoshan Wang
- Chapter 6 **Stopped-Flow Studies of the Formation of Organic Nanocrystals in the Reprecipitation Method** 165
Daniel Oliveira, Koichi Baba, Winfried Teizer, Hitoshi Kasai
Hidetoshi Oikawa and Hachiro Nakanishi
- Chapter 7 **Self-assembly and Patterning of Nanocrystals** 185
Yoshitake Masuda
- Chapter 8 **Synthesis and Characterization of Dispersion Reinforced Sintered System Based on Ultra Fine and Nanocomposite $\text{Cu-Al}_2\text{O}_3$ Powders** 217
Zoran Anđić, Aleksandar Vujović, Miloš Tasić,
Marija Korać and Željko Kamberović

- Chapter 9 **Alkaline-Earth Metal Carbonate, Hydroxide and Oxide Nano-Crystals Synthesis Methods, Size and Morphologies Consideration** 237
 Mohammad Amin Alavi and Ali Morsali
- Part 2 Nanostructuring and Function of Nanocrystals** 263
- Chapter 10 **Nano/Micro-Patterning of Metal Oxide Nanocrystals** 265
 Yoshitake Masuda
- Chapter 11 **Designing Nanocrystal Electrodes by Supercritical Fluid Process and Their Electrochemical Properties** 293
 Dinesh Rangappa and Itaru Honma
- Chapter 12 **Photoelectron and Photosensitization Properties of Silicon Nanocrystal Ensembles** 313
 Elizaveta A. Konstantinova, Vyacheslav A. Demin and Pavel K. Kashkarov
- Chapter 13 **Magnetic Nanostructures for Biomedical Applications: An Iron Nitride Crystal/Cationic Lipid Nanocomposite for Enhanced Magnetically Guided RNA Interference in Cancer Cells** 349
 Yoshihisa Namiki, Satoshi Matsunuma, Tetsutaro Inoue, Shigeo Koido, Akihito Tsubota, Yoji Kuse and Norio Tada
- Chapter 14 **Tailoring the Morphology and the Optical Properties of Semiconductor Nanocrystals by Alloying** 373
 Young-Kuk Kim and Chul-Jin Choi
- Chapter 15 **Functional Organic Nanocrystals** 397
 Koichi Baba, Hitoshi Kasai, Kohji Nishida and Hachiro Nakanishi
- Chapter 16 **Structure of Nanocrystals in Finemets with Different Silicon Content and Stress-Induced Magnetic Anisotropy** 415
 Nikolay V. Ershov, Yuri P. Chernenkov, Vladimir I. Fedorov, Vera A. Lukshina, Nadezda M. Kleinerman, Vadim V. Serikov, Anatoly P. Potapov and Nikita K. Yurchenko
- Chapter 17 **Energy Transfer from Silicon Nanocrystals to Er^{3+} Ions Embedded in Silicon Oxide Matrix** 437
 Kantisara Pita and Quang Vinh Vu
- Chapter 18 **Nonlinear Optoelectronic Devices Based on Nanocrystalline Silicon Films: Acoustoelectrical Switchers for Optical Modes, Nonlinear Optical Switchers and Lasers** 459
 Dmitry E. Milovzorov

Preface

Nanocrystals have been attracting much attention for future science and technology. Chapters are sought that address innovative solutions to the design, synthesis, crystallization, morphology control, self-assembly, nano/micro-structure formation, patterning, novel property and device application of Nanocrystals. The book involves Nanocrystals of metal oxides, semiconductors, compounds, noble metals, metals, inorganic materials, carbon materials, organic molecules, polymers, bio materials, hybrid materials, composites, etc. It features remarkable breakthrough on Nanocrystals and provides latest scientific knowledge and leading-edge technology. They offer research agenda and accelerate the research, development and diffusion of Nanocrystals.

In closing, I wish to express my sincere sense of gratitude to the authors, publishing process manager Ms. Silvia Vlase, and the publishing staff. I dedicate this book to my parents, Mr. Toshio Masuda and Ms. Nobuko Masuda, my sisters, Ms. Shinobu Horita and Ms. Satoe Amaya, my children, Ms. Yuuka Masuda, Ms. Arisa Masuda and Mr. Ikuto Masuda, and my wife, Ms. Yumi Masuda.

Yoshitake Masuda

National Institute of Advanced Industrial Science and Technology (AIST),
Japan

Part 1

Synthesis and Design of Nanocrystals

Morphology Control of Metal Oxide Nanocrystals

Yoshitake Masuda

*National Institute of Advanced Industrial Science and Technology (AIST)
Anagahora, Shimoshidami, Moriyama-ku, Nagoya
Japan*

1. Introduction

Metal oxides have been widely used in electro devices, optical devices, etc. Recently, liquid phase syntheses of them attract much attention as future technology and novel academic field. Especially, liquid phase syntheses of anisotropic particles or films are expected for next generation metal oxide devices. This section describes liquid phase morphology control of anisotropic metal oxide. They were realized by precise control of nucleation and crystal growth. They showed high performance of solution systems for future metal oxide devices. Liquid phase morphology control of anisotropic metal oxide particles and films would contribute to development of metal oxide science and technology.

2. Morphology control of acicular BaTiO₃ particles¹

Acicular BaTiO₃ particles were developed using solution systems. The morphology of BaC₂O₄ · 0.5H₂O was controlled to acicular shape. Its phase transition to BaTiO₃ was realized by introducing Ti ions from the coprecipitated amorphous phase. Acicular BaTiO₃ particles have an aspect ratio as high as 18 and the particle size can be controlled by varying the growth period of BaC₂O₄ · 0.5H₂O which governs the size of BaC₂O₄ · 0.5H₂O particles. Acicular particles of crystalline BaTiO₃ can be used for ultra-thin multilayer ceramic capacitors.

Multilayer ceramic capacitors (MLCC) are indispensable electronic components for advanced electronic technology²⁻¹², but larger capacity and smaller size are needed for future electronic devices. To meet these needs, BaTiO₃ particles were downsized, but ferroelectric ceramics lose their ferroelectricity when their particle size is decreased and lose ferroelectricity entirely at a critical size²⁻¹¹. This is known as the size effect and it impedes the progress of MLCC, so a novel solution has been eagerly anticipated.

Here, we propose MLCC using acicular BaTiO₃ particles¹³. An ultra-thin ferroelectric layer and high capacity can be realized by acicular particles having a high aspect ratio. The short side provides an ultra-thin ferroelectric layer and the large volume caused by the long side avoids the loss of ferroelectricity at the critical size. Anisotropic BaTiO₃ particles are thus a candidate for MLCC. BaTiO₃ has, however, an isotropic cubic or tetragonal structure, and its morphology is extremely difficult to control due to its isotropic crystal faces. We focused on triclinic BaC₂O₄ · 0.5H₂O which has an anisotropic crystal structure and controlled the morphology of these particles by precisely controlling crystal growth. We also achieved

phase transition of $\text{BaC}_2\text{O}_4 \cdot 0.5\text{H}_2\text{O}$ to crystalline BaTiO_3 by introducing Ti ions from the coprecipitated amorphous phase. Having developed several key technologies, we were successfully able to produce anisotropic acicular BaTiO_3 particles.

Morphology control of BaTiO_3 to rod-shape was reported previously. Additionally, metal oxalates (MC_2O_4) have been used for synthesis of rod-shaped oxides or hydroxides. Y. Hayashi *et al.* reported preparation of rod-shaped BaTiO_3 from rod-shaped $\text{TiO}_2 \cdot n\text{H}_2\text{O}$ and BaCO_3 in molten chloride at high temperature¹⁴. Li *et al.* reported preparation of nanoflakes and nanorods of $\text{Ni}(\text{OH})_2$, $\text{Co}(\text{OH})_2$ and Fe_3O_4 by hydrothermal conversion at 160 °C for 12 h from $\text{MC}_2\text{O}_4 \cdot 2\text{H}_2\text{O}$ in NaOH solutions¹⁵. Sun *et al.* prepared flowerlike SnC_2O_4 submicrotubes in ethanol solutions containing SnCl_2 and oxalic acid. They were annealed at 500 °C for 2 h in ambient atmosphere to obtain flowerlike SnO_2 submicrotubes¹⁶.

Oxalic acid (252 mg) was dissolved into isopropyl alcohol (4 ml) (Fig. 1)¹. Butyl titanate monomer (0.122 ml) was mixed with the oxalic acid solution, and the solution was then mixed with distilled water (100 ml). The pH of the solution was increased to pH = 7 by adding NaOH (1 M) and distilled water, while the volume of the solution was adjusted to 150 ml by these additions. The aqueous solution (50 ml) with barium acetate (39.3 mg) was mixed with the oxalic acid solution. The mixed solution containing barium acetate (0.77 mM), butyl titanate monomer (2 mM) and oxalic acid (10 mM) was kept at room temperature for several hours with no stirring, and the solution gradually became cloudy. Stirring causes the collision of homogeneously nucleated particles and destruction of large grown particles, and so was avoided in this process. The size of the precipitate was easily controlled from nanometer order to micrometer order by changing the growth period. Large particles were grown by immersion for several hours to evaluate the morphology and crystallinity in detail.

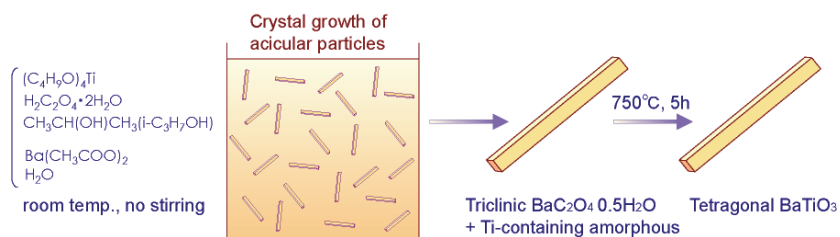


Fig. 1. Conceptual process for fabricating acicular BaTiO_3 particles. Morphology control of $\text{BaC}_2\text{O}_4 \cdot 0.5\text{H}_2\text{O}$ particles and phase transition to BaTiO_3 . Reprinted with permission from Ref.¹, Masuda, Y., Yamada, T. and Koumoto, K., 2008, *Cryst. Growth Des.*, 8, 169. Copyright ©American Chemical Society

Oxalate ions ($\text{C}_2\text{O}_4^{2-}$) react with barium ions (Ba^{2+}) to form barium oxalate ($\text{BaC}_2\text{O}_4 \cdot 0.5\text{H}_2\text{O}$). $\text{BaC}_2\text{O}_4 \cdot 0.5\text{H}_2\text{O}$ is dissolved in weak acetate acid provided by barium acetate ($(\text{CH}_3\text{COO})_2\text{Ba}$), however, it can be deposited at pH 7 which is adjusted by adding NaOH. $\text{BaC}_2\text{O}_4 \cdot 0.5\text{H}_2\text{O}$ was thus successfully precipitated from the solution.

Acicular particles were homogeneously nucleated and precipitated from the solution. They were on average 23 μm (ranging from 19 to 27 μm) in width and 167 μm (ranging from 144 to 189 μm) in length, giving a high aspect ratio of 7.2 (Fig. 2). They had sharp edges and clear crystal faces, indicating high crystallinity. A gel-like solid was also coprecipitated from the solution as a second phase.

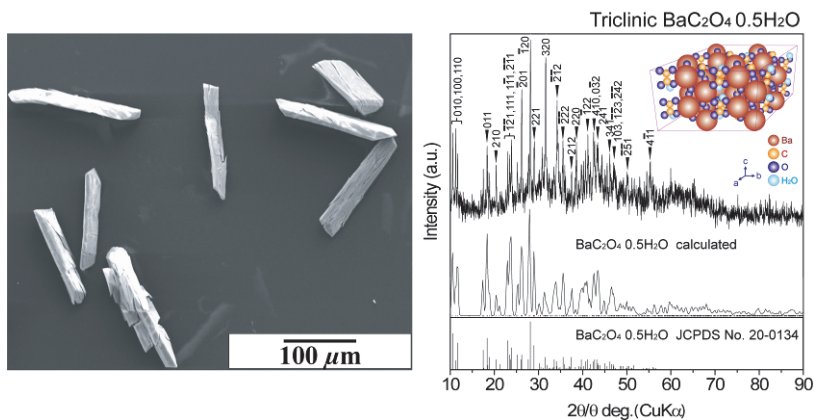


Fig. 2. SEM micrograph and XRD diffraction pattern of acicular $\text{BaC}_2\text{O}_4 \cdot 0.5\text{H}_2\text{O}$ particles precipitated from an aqueous solution at pH = 7. XRD diffraction measurement data (first step), XRD pattern calculated from crystal structure data¹⁶ (second step) and XRD pattern of JCPDS No. 20-134 (third step) are shown for triclinic $\text{BaC}_2\text{O}_4 \cdot 0.5\text{H}_2\text{O}$. Reprinted with permission from Ref.¹, Masuda, Y., Yamada, T. and Koumoto, K., 2008, *Cryst. Growth Des.*, 8, 169. Copyright ©American Chemical Society

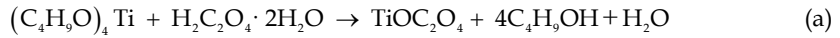
XRD diffraction patterns for the mixture of acicular particles and gel-like solid showed sharp diffraction peaks of crystalline $\text{BaC}_2\text{O}_4 \cdot 0.5\text{H}_2\text{O}$ with no additional phase. Acicular particles were crystalline $\text{BaC}_2\text{O}_4 \cdot 0.5\text{H}_2\text{O}$ and the gel-like solid would be an amorphous phase.

Fortunately, $\text{BaC}_2\text{O}_4 \cdot 0.5\text{H}_2\text{O}$ has a triclinic crystal structure as shown by the model calculated from structure data¹⁷ (Fig. 2 XRD first step) and thus anisotropic crystal growth was allowed to proceed to produce an acicular shape. Each crystal face has a different surface energy and surface nature such as zeta potential and surface groups. Anisotropic crystal growth is induced by minimizing the total surface energy in ideal crystal growth. Additionally, site-selective adsorption of ions or molecules on specific crystal faces suppresses crystal growth perpendicular to the faces and so induces anisotropic crystal growth. These factors would cause anisotropic crystal growth of $\text{BaC}_2\text{O}_4 \cdot 0.5\text{H}_2\text{O}$ and hence allow us to control morphology and fabricate acicular $\text{BaC}_2\text{O}_4 \cdot 0.5\text{H}_2\text{O}$ particles. The positions of diffraction peaks corresponded with that of JCPDS No. 20-0134 (Fig. 2 XRD third step) and that calculated from crystal structure data¹⁷ (Fig. 2 XRD second step), however, several diffraction peaks, especially 320 and 201, were enhanced strongly compared to their relative intensity. The enhancement of diffraction intensity from specific crystal faces would be related to anisotropic crystal growth; a large crystal size in a specific crystal orientation increases the x-ray diffraction intensity for the crystal face perpendicular to the crystal orientation.

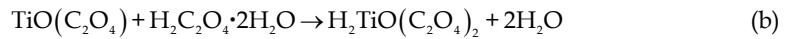
EDX elemental analysis indicated the chemical ratio of the precipitate, which included acicular particles and gel-like solid, to be about Ba / Ti = 1 to 1.5. The chemical ratio indicated that the coprecipitated amorphous gel contained Ti ions. Additional Ba ions can be transformed into BaCO_3 by annealing and removed by HCl treatment in the next step. The ratio was thus controlled to slightly above Ba / Ti = 1 by adjusting the volume ratio of acicular particles and gel-like solid. Consequently, acicular particles of crystalline $\text{BaC}_2\text{O}_4 \cdot$

0.5H₂O with Ti-containing gel-like solid were successfully fabricated in an aqueous solution process.

In comparison, isotropic particles of barium titanyl oxalate (BaTiO(C₂O₄)₂ · 4H₂O) were precipitated at pH 2. TiOC₂O₄ was formed by the following reaction in which the reaction of oxalic acid (H₂C₂O₄ · 2H₂O) with butyl titanate monomer ((C₄H₉O)₄Ti) and hydrolysis can take place simultaneously¹⁸.



TiO(C₂O₄) was then converted to oxalotitanic acid (H₂TiO(C₂O₄)₂) by the reaction:



Alcoholic solution containing oxalotitanic acid (H₂TiO(C₂O₄)₂) formed by reaction (b) was subjected to the following cation exchange reaction by rapidly adding an aqueous solution of barium acetate at room temperature:



BaTiO(C₂O₄)₂ isotropic particles were formed by reaction (c).

On the other hand, neither BaC₂O₄ · 0.5H₂O nor BaTiO(C₂O₄)₂ was precipitated at pH 3 to pH 6. Gel-like solid was formed in the solution and their XRD spectra showed no diffraction peaks. The amorphous gel that precipitated at pH = 3 to 6 would be the same as the amorphous gel coprecipitated at pH 7.

These comparisons show that the crystal growth and morphology control of BaC₂O₄ · 0.5H₂O are sensitive to the solution conditions.

The precipitate was annealed at 750 °C for 5 h in air. Acicular BaC₂O₄ · 0.5H₂O particles were reacted with Ti-containing amorphous gel to introduce Ti ions to transform into crystalline BaTiO₃. X-ray diffraction of the annealed precipitate showed crystalline BaTiO₃ and an additional barium carbonate phase (BaCO₃). Excess precipitation of BaC₂O₄ · 0.5H₂O caused the generation of barium carbonate phase (BaCO₃) as expected.

The annealed precipitate was further immersed in HCl solution (1 M) to dissolve barium carbonate (BaCO₃). Acicular particles of crystalline BaTiO₃ were successfully fabricated with no additional phase. Particles showed acicular shape with 2.8×10×50 μm and x-ray diffraction of single-phase crystalline BaTiO₃ (Fig. 3). The high aspect ratio of the particles (17.8 = 50 / 2.8) would be provided by that of BaC₂O₄ · 0.5H₂O particles. The particle size of acicular BaTiO₃ can be easily controlled by the growth period and solution concentration for BaC₂O₄ · 0.5H₂O precipitation which decides the particle size of BaC₂O₄ · 0.5H₂O.

BaTiO₃ has a cubic crystal structure at high temperature above phase transition and has a tetragonal crystal structure at room temperature. The cubic crystal structure is completely isotropic and the tetragonal crystal structure results from stretching a cubic lattice along one of its lattice vectors. For both of the crystal structures it is difficult to control anisotropic crystal growth, however, with our newly developed process we could successfully control the morphology and fabricate acicular particles. This was achieved by controlling the morphology of triclinic BaC₂O₄ · 0.5H₂O to acicular shape and the phase transition to BaTiO₃ by introducing Ti ions from the coprecipitated amorphous phase. The novel concept can be applied to a wide variety of morphology control and crystal growth control for advanced electronic devices composed of crystalline materials.

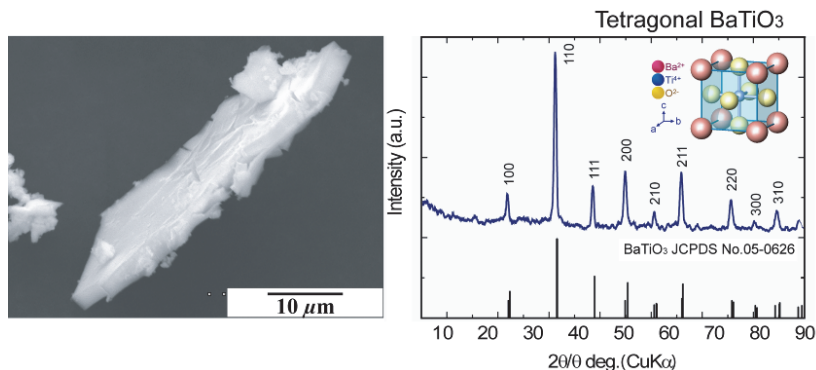
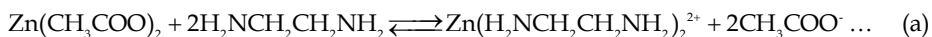


Fig. 3. SEM micrograph and XRD diffraction pattern of acicular BaTiO₃ particles after annealing at 750 °C for 5 h and HCl treatment. XRD diffraction measurement data (first step) and XRD pattern of JCPDS No. 05-0626 (second step) are shown for tetragonal BaTiO₃. Reprinted with permission from Ref.¹, Masuda, Y., Yamada, T. and Koumoto, K., 2008, *Cryst. Growth Des.*, 8, 169. Copyright @American Chemical Society

3. Morphology control of ZnO particles^{19,20}

Ethylenediamine (H₂N-CH₂CH₂-NH₂, 15–45 mM, Sigma-Aldrich) was added to the zinc acetate aqueous solution (Zn(CH₃COO)₂, 15 mM, Kishida Chemical Co., Ltd.) to promote deposition of ZnO¹⁹. Zinc chelate (Zn(H₂N-CH₂CH₂-NH₂)₂²⁺) was formed from zinc acetate and ethylenediamine in reaction (a). ZnO was crystallized from zinc chelate and hydroxide ion (OH⁻) in reaction (c).



The solution became turbid shortly after adding ethylenediamine. The molar ratio of ethylenediamine to Zn was [ethylenediamine] / [Zn] = (a) 1 : 1, (b) 2 : 1 or (c) 3 : 1. pH of the solutions were (a) pH=7.3, (b) pH=8.0 or (c) pH=8.7, respectively. Crystal growth rate and deposition of ZnO were attempted to control to change particle morphology. Si substrate (Newwingo Co., Ltd.) was immersed to evaluate deposited ZnO particles and particulate films. The solution in a glass beaker was kept at 60 °C for 3 h using a water bath. The silicon substrate was cleaned before immersion as described in references. The substrate was rinsed with distilled water after immersion.

ZnO particles having hexagonal cylinder shape were homogeneously nucleated and deposited in the aqueous solution containing 15 mM ethylenediamine ([ethylenediamine] / [Zn] = (a) 1 : 1) (Fig. 4a). X-ray diffraction patterns showed the deposition to be well crystallized ZnO (Fig. 5a). The relative intensity of (10-10) and (0002) is similar to that of randomly deposited ZnO particles, indicating the random orientation of deposited ZnO

Thank You for previewing this eBook

You can read the full version of this eBook in different formats:

- HTML (Free /Available to everyone)
- PDF / TXT (Available to V.I.P. members. Free Standard members can access up to 5 PDF/TXT eBooks per month each month)
- Epub & Mobipocket (Exclusive to V.I.P. members)

To download this full book, simply select the format you desire below

